

# Phase Sensitive Detection of 2D Homonuclear Correlation Spectra in MAS NMR

G. J. Boender\*<sup>†</sup> and S. Vega\*

\*Department of Chemical Physics, Weizmann Institute of Science, 76100 Rehovot, Israel; and <sup>†</sup>Faculteit der Natuurwetenschappen, Fysische Chemie, Katholieke Universiteit Nijmegen, Toernooiveld 1, 6525 ED Nijmegen, The Netherlands

Received December 16, 1997; revised March 27, 1998

**A pulse scheme for phase sensitive detection of two-dimensional (2D) homonuclear correlation magic angle spinning (MAS) NMR spectra is proposed. This scheme combines the time proportional phase increment phase cycling scheme and the time reversal 2D MAS experiment. This approach enables the direct detection of purely absorptive 2D MAS spectra, containing cross peaks that connect only diagonal peaks of dipolar correlated spins.** © 1998 Academic Press

**Key Words:** magic angle spinning NMR; phase sensitive; time reversal; homonuclear correlation; spectroscopy; time proportional phase increment.

## 1. INTRODUCTION

The introduction of the rotor frequency-driven dipolar recoupling (RFDR) sequence has provided a simple strategy for the detection of two-dimensional (2D) homonuclear dipolar correlation spectra in magic angle spinning (MAS) NMR of uniformly enriched molecules in polycrystalline materials (1). This approach was extended by using a variety of new techniques, such as RIL and TOBSY, which have resulted in similar and improved results (2–4). The analysis of the 2D correlation spectra can assist in structure determination of systems that are inaccessible by diffraction techniques (5, 6). Absorption lineshapes of the diagonal and cross peaks in 2D spectra are a requirement for optimal resolution in these spectra. In 1D NMR, quadrature detection enables one to obtain pure absorption lineshapes by phase correction of the Fourier-transformed spectra (7). In 2D NMR spectroscopy, the time proportional phase increment (TPPI) phase cycling scheme can provide absorptive lineshapes in both dimensions (8). In this procedure the  $t_1$  dependence of the 2D signal reflects itself as an amplitude modulation of the  $t_2$  acquisition signal components,  $\cos(\omega_1 t_1 + \omega_T t_1) \exp(i\omega_2 t_2)$ , with  $\omega_1$  and  $\omega_2$  resonance frequencies and  $\omega_T$  a frequency shift equal to half the Nyquist frequency. Fourier transformation separates the spectral lines of the echo and anti-echo signals by  $\omega_T$  and results in the absorption lineshapes (7, 9).

When the TPPI approach is applied to solid samples rotating at the magic angle, the signals in the 2D magic angle spinning NMR

experiment do not consist of simple  $\cos(\omega_1 t_1 + \omega_T t_1) \exp(i\omega_2 t_2)$  terms, leading to auto-cross peaks between the center and sidebands due to the chemical shift anisotropy, as well as nonpure absorptive lineshapes (10). These cross peaks complicate the 2D MAS spectra and cause unwanted signal intensity distributions lowering the spectral resolution. To eliminate the auto-cross peaks in 2D MAS exchange NMR measurements, De Jong *et al.* suggested synchronizing the mixing time with the sample rotation (11). To obtain pure absorption lines, Hagemeyer *et al.* combined 2D spectra measured using this synchronization with 2D spectra using a time reversal scheme (10, 12–14).

In this article the time reversal experiment is combined with the TPPI method in order to detect directly in one single experiment phase sensitive 2D MAS homonuclear correlation spectra with absorption lineshapes of fully  $^{13}\text{C}$  enriched solid compounds.

## 2. RESULTS AND DISCUSSION

The pulse scheme of the 2D MAS NMR correlation spectroscopy is presented in Fig. 1. All experiments were performed on a crystalline  $[\text{U-}^{13}\text{C}]\text{L-tyrosine} \cdot \text{HCl}$  sample. In a standard TPPI 2D correlation NMR experiment, the evolution time  $t_1$  dependence of the signal  $S(t_1, t_2)$  components equals to the sum of time dependent (+1) quantum coherences  $\{\exp(-i\omega_1 t_1)\}$  and (-1) quantum coherences  $\{\exp(i\omega_1 t_1)\}$  of the spin system

$$\cos(\omega_1 t_1 + \omega_T t_1) \exp(i\omega_2 t_2), \quad [1]$$

while the (-1) coherence is monitored during the detection period  $t_2$ . After the Fourier transformation these echo and the anti-echo components are separated from each other by a frequency  $\omega_T$ , equal to half the Nyquist frequency (7).

In MAS NMR, the chemical shift anisotropies (CSA) of the observed spins complicate the spectra by generating sidebands flanking the centerbands. The FID of a single spin, with a CSA tensor with Euler angles  $(\alpha, \beta, \gamma)$  in the rotor frame, can be written as  $f^*(\gamma) f(\gamma + \omega_r t)$ , with  $f(x)$  a function of the form  $\sum_n d_n \exp(inx)$  (13). In this expression the isotropic shift is

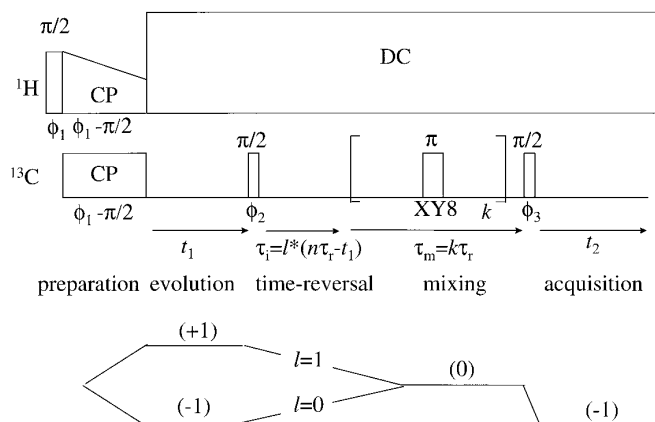


**FIG. 1.** Schematic representation of the phase-sensitive RFDR pulse sequence used for the absorption mode 2D MAS dipolar correlation experiments. Relevant rotation angles are depicted on top of the corresponding pulse, while the RF phases are indicated beneath the pulses. The entire  $^1\text{H}$ - $^{13}\text{C}$  RAMP preparation phase  $\phi_1$  was varied following the TPPI scheme. An XY-8 train of rotor-synchronized  $\pi$ -pulses was applied during the mixing time. Coherence transfer pathway selection, ring-down elimination, and time reversal were attained by cycling of the phases  $\phi_2$ ,  $\phi_3$ , and  $\phi_{\text{ref}}$  and switching between the non-time-reversed ( $l = 0$ ) and time-reversed ( $l = 1$ ) experiments, as listed in Table 1.  $t_1$  and  $t_2$  indicate the evolution and acquisition time, respectively, according to the standard convention.

omitted and the coefficients  $d_n$  are functions of all parameters defining the CSA tensor, except  $\gamma$ . The signal of the anti-echo part of the 2D TPPI MAS NMR experiment on this spin has the form

$$(f^*(\gamma)f(\gamma + \omega_r t_1))(f^*(\gamma + \omega_r t_1)f(\gamma + \omega_r t_1 + \omega_r t_2)) \quad [2]$$

and the echo signal becomes

$$f(\gamma)f^*(\gamma + \omega_r t_1)f^*(\gamma + \omega_r t_1)f(\gamma + \omega_r t_1 + \omega_r t_2), \quad [3]$$

where the additional coefficients  $\exp(i\omega_r t_1)$  and  $\exp(-i\omega_r t_1)$  generated by the TPPI phase cycling, respectively, are omitted. In these expressions it is assumed that the length of the mixing time is equal to an integer multiple of the spinning period  $N\tau_r$ , according to De Jong *et al.* (11). In these formulae no cross correlation and relaxation processes during this time are taken into account. Integration over  $\gamma$ , needed to obtain the signal of a powder sample, results in the anti-echo signal

$$\sum_n d_n^* d_n \exp\{in\omega_r(t_1 + t_2)\} \quad [4]$$

and the echo signal

$$\sum_{l,m,n} d_{m-l+n}^* d_m^* d_n \exp\{-im\omega_r t_1\} \exp\{in\omega_r t_2\}, \quad [5]$$

where we used that

$$f(x)f^*(x) = 1 \quad \text{and} \quad \frac{1}{2\pi} \int_0^{2\pi} d\gamma \exp(in\gamma) = \delta_{k0}.$$

Addition of these signals, according to the TPPI procedure, will not result in a sum of terms of the form of Eq. [1] and therefore will not result in pure absorptive peaks in the 2D spectrum. In Fig. 2 the 2D spectrum of this TPPI experiment is shown. As can be seen in this figure, some of the diagonal peaks do not exhibit absorption lineshapes. In addition auto-cross peaks between center and sidebands are present that are not eliminated by the phase cycling. Only those centerbands, which have CSA tensor values smaller than the spinning speed, are absorptive and do not show auto-cross peaks. To obtain pure absorption for all diagonal peaks and to eliminate the auto-cross peaks the anti-echo experiment must be combined with an echo time reversal experiment, in which the mixing time is reduced by an amount equal  $t_1$ , as suggested by Hagemeyer *et al.* (13). The echo time reversal experiment gives a 2D signal of the form

$$f(\gamma)f^*(\gamma + \omega_r t_1)f^*(\gamma)f(\gamma + \omega_r t_2), \quad [6]$$

while the corresponding anti-echo experiment results in a signal of the form

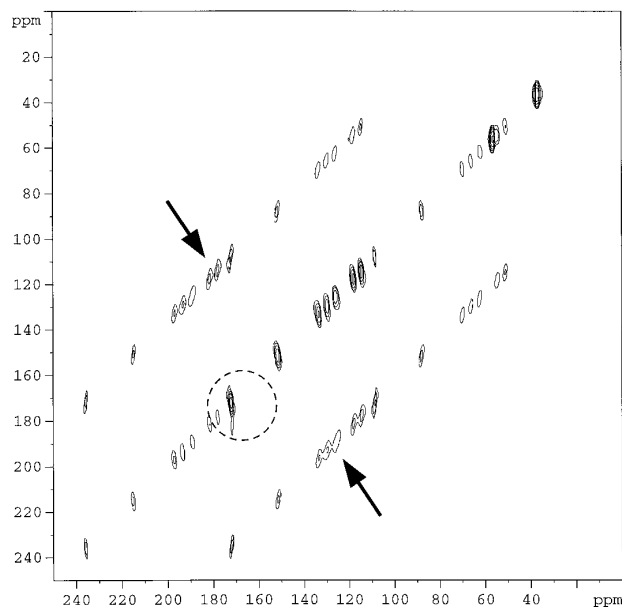


**FIG. 2.** Contour plot of a 2D MAS spectrum of  $[\text{U-}^{13}\text{C}]\text{Tyrosine} \cdot \text{HCl}$  collected with the pulse sequence of Fig. 1, without time reversal ( $l = 0$ ) at a spinning speed  $\omega_r/2\pi = 8000 \pm 4$  Hz with  $\tau_m = 0$ . The circle indicates a nonabsorption lineshape, while the arrows indicate the lines of auto-cross peaks.

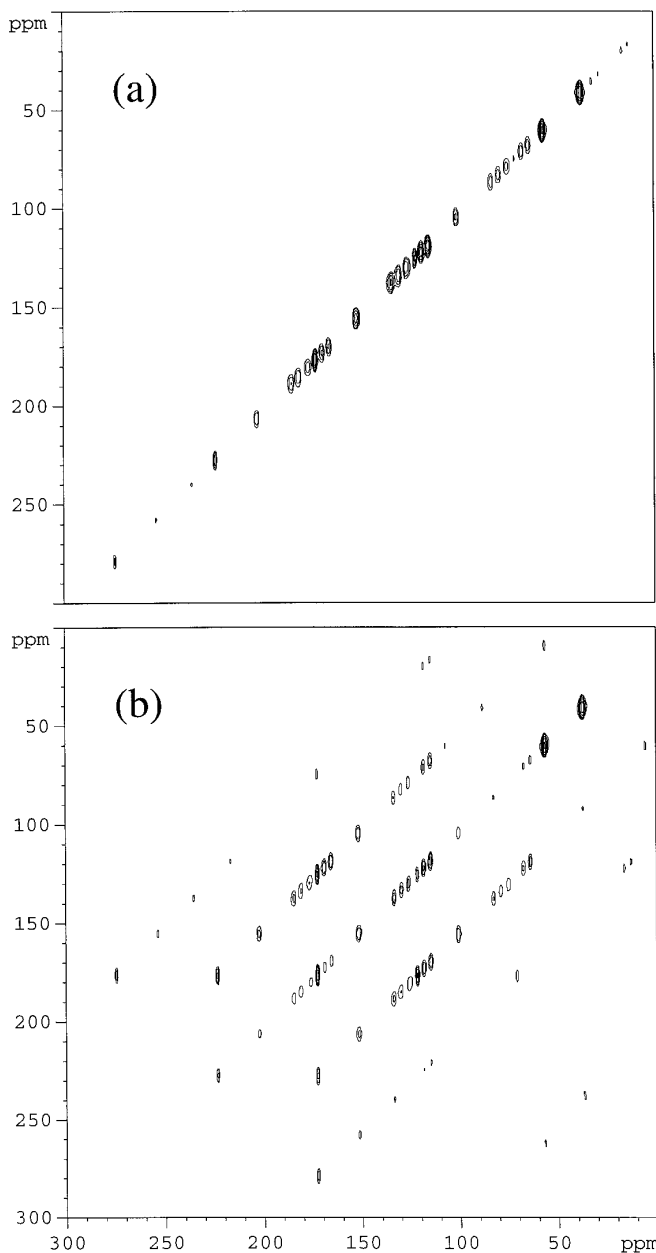


**FIG. 3.** Contour plots of absorption mode 2D MAS spectra of  $[U-^{13}C]$ Tyrosine · HCl collected with the pulse sequence of Fig. 1, with  $\omega_r/2\pi = 6400 \pm 3$  Hz and  $\tau_m = 0$ . For (a) the anti-echo experiment without time reversal ( $0 \rightarrow -1 \rightarrow l = 0 \rightarrow 0 \rightarrow -1$ ) is combined with the echo experiment with time reversal ( $0 \rightarrow +1 \rightarrow l = 1 \rightarrow 0 \rightarrow -1$ ), and for (b) the anti-echo experiment with time reversal ( $0 \rightarrow -1 \rightarrow l = 1 \rightarrow 0 \rightarrow -1$ ) is combined with the echo experiment without time reversal ( $0 \rightarrow +1 \rightarrow l = 0 \rightarrow 0 \rightarrow -1$ ).

$$f^*(\gamma)f(\gamma + \omega_r t_1)f^*(\gamma)f(\gamma + \omega_r t_2). \quad [7]$$

The  $\gamma$ -integrated signals become

$$\sum_n d_n^* d_n \exp\{in\omega_r(-t_1 + t_2)\} \quad [8]$$

for the echo experiment and

$$\sum_{l,m,n} d_{m-l+n}^* d_l^* d_m d_n \exp\{im\omega_r t_1\} \exp\{in\omega_r t_2\}, \quad [9]$$

for the anti-echo experiment, respectively. The addition of the anti-echo and echo signals in Eqs. [4] and [8] yields

$$\sum_n d_n^* d_n \cos\{n\omega_r t_1\} \exp\{in\omega_r t_2\} \quad [10]$$

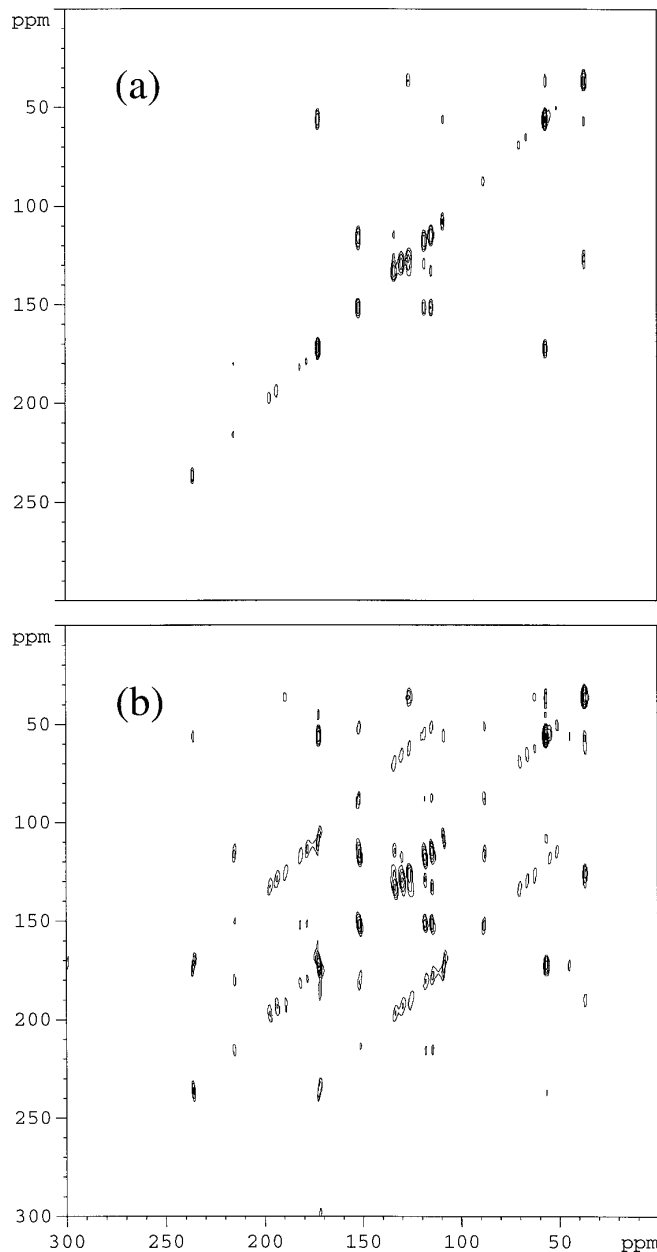


**FIG. 4.** Contour plots of absorption mode 2D MAS dipolar correlation spectra of  $[U-^{13}C]$ Tyrosine · HCl collected with the pulse sequence of Fig. 1 and the phase cycle shown in Table 1, with  $\omega_r/2\pi = 8000 \pm 4$  Hz and  $\tau_m = 8\tau_r$ . The contours (a) and (b) were obtained with and without time reversal ( $0 \rightarrow \pm 1 \rightarrow l = 0 \rightarrow 0 \rightarrow -1$ ), respectively.

TABLE 1

Step	1	2	3	4	5	6	7	8	9	10	11	12	13	14	15	16
$l$	0	0	0	0	0	0	0	0	0	0	0	0	0	0	0	0
$\phi_2$	0	0	0	0	$\pi$	$\pi$	$\pi$	$\pi$	$\pi/2$	$\pi/2$	$\pi/2$	$\pi/2$	$3\pi/2$	$3\pi/2$	$3\pi/2$	$3\pi/2$
$\phi_3$	0	$\pi/2$	$\pi$	$3\pi/2$	0	$\pi/2$	$\pi$	$3\pi/2$	$\pi/2$	$\pi$	$3\pi/2$	0	$\pi/2$	$\pi$	$3\pi/2$	0
$\phi_{\text{ref}}$	0	$\pi/2$	$\pi$	$3\pi/2$	$\pi$	$3\pi/2$	0	$\pi/2$	0	$\pi/2$	$\pi$	$3\pi/2$	$\pi$	$3\pi/2$	0	$\pi/2$
Step	17	18	19	20	21	22	23	24	25	26	27	28	29	31	30	32
$l$	1	1	1	1	1	1	1	1	1	1	1	1	1	1	1	1
$\phi_2$	0	0	0	0	$\pi$	$\pi$	$\pi$	$\pi$	$\pi/2$	$\pi/2$	$\pi/2$	$\pi/2$	$3\pi/2$	$3\pi/2$	$3\pi/2$	$3\pi/2$
$\phi_3$	0	$\pi/2$	$\pi$	$3\pi/2$	0	$\pi/2$	$\pi$	$3\pi/2$	$3\pi/2$	0	$\pi/2$	$\pi$	$3\pi/2$	$\pi/2$	0	$\pi$
$\phi_{\text{ref}}$	0	$\pi/2$	$\pi$	$3\pi/2$	$\pi$	$3\pi/2$	0	$\pi/2$	0	$\pi/2$	$\pi$	$3\pi/2$	$\pi$	0	$3\pi/2$	$\pi/2$

Note. This 32-step phase cycle is used to obtain absorption mode 2D MAS dipolar correlation spectra. The phase angles correspond to those depicted in Fig. 1.  $\phi_1$  takes care of the TPPI scheme. For each increment of  $t_1$  this phase, representing the phases of pulses in the entire preparation period, is incremented by  $\pi/2$ .  $\phi_2$  is used for ring-down elimination, while  $\phi_3$  and  $\phi_{\text{ref}}$  are used for zero quantum filtration.  $\phi_2$  and  $\phi_3$  are also used to select first the anti-echo ( $0 \rightarrow -1 \rightarrow 0 \rightarrow -1$ ), and in the second part of the cycle the echo ( $0 \rightarrow +1 \rightarrow 0 \rightarrow -1$ ) signals (7). The value of 1 represents the non-time-reversal experiments ( $l = 0$ ) with  $\tau_m = k\tau_r$ , and the time reversal experiments ( $l = 1$ ) with  $\tau_m = k\tau_r - t_1$ .

and of Eqs. [5] and [9] gives

$$\sum_{l,m,n} d_{m-l+n}^* d_l^* d_m d_n \cos\{in\omega_r t_1\} \exp\{in\omega_r t_2\}. \quad [11]$$

Both of these signals are equal to a sum of cosine-exponent terms, resulting in pure absorption lines, but only Eq. [10] does not result in any auto-cross peaks. The time reversal TPPI MAS experiments corresponding to Eqs. [10] and [11] are shown in Fig. 3. Only the combination of the anti-echo with the time-reversed echo signals results in a pure absorption spectrum free of auto-cross peaks. The 32-phase cycle of the proper time reversal TPPI experiment is presented in Table 1. This phase cycling scheme is used to obtain the homonuclear correlation spectrum shown in Fig. 4a. For comparison, the spectrum obtained by a standard TPPI MAS experiment is shown in Fig. 4b.

From these spectra it can be concluded that with the method presented in this paper, one can obtain pure absorption 2D correlation spectra in a single experiment by combining TPPI with the time reversal experiment. The resulting 2D spectra exhibit cross peaks only between the diagonal peaks of correlated spins as well as center and sideband signals that are all purely absorptive. Therefore, this strategy enhances the spectral resolution and sensitivity, which helps to improve the strategy of structure elucidation using 2D MAS NMR correlation spectra.

### 3. EXPERIMENTAL

Uniformly  $^{13}\text{C}$  enriched tyrosine was obtained from Cambridge Isotope Laboratories. The HCl salt was prepared by dissolving the tyrosine in 1M HCl in  $\text{H}_2\text{O}$ , followed by evaporation of the solvent.

All NMR experiments were performed on a DMX500 Bruker spectrometer, equipped with a double-tuned 4-mm CP/MAS

probe. The tyrosine was packed in a 4-mm rotor, using 2.5-mm spacers to reduce the effective RF inhomogeneity over the sample. Spectra were collected with a sweep width of 50 kHz at a spinning speed of 6.2 kHz  $< \omega_r/2\pi < 8$  kHz. The  $^{13}\text{C}$  nutation frequency was 60 kHz. RAMP cross polarization with a contact time of 2 ms was used (15). The cycle time between scans was typically 1 s and data were acquired under TPPM  $^1\text{H}$  heteronuclear dipolar decoupling with a phase-modulation angle of  $18^\circ$ , while the flip pulse length of 6.2  $\mu\text{s}$  was adjusted to yield optimal  $^{13}\text{C}$  resolution (16). The offset between the cross polarization and decoupling power was 3 dB. During the mixing time  $\pi$ -pulses were applied in the middle of the rotor period in order to recouple the dipolar interactions between the carbons and XY-8 phase cycling was used (1, 17). The FIDS were recorded with 2k data points and 128 points in the  $t_1$  dimension were recorded. The data was zero filled up to a 2k in both dimensions. In the  $t_1$  dimension a sine-square apodization, shifted by  $\pi/2$ , was used prior to Fourier transformation and in the  $t_2$  dimension a Lorentzian broadening of 10 Hz was applied.

### ACKNOWLEDGMENTS

This research was supported by the Netherlands Organisation for Scientific Research (NWO). We thank Professor Z. Luz for stimulating discussions on the subject of time reversal MAS NMR.

### REFERENCES

1. A. E. Bennett, J. H. Ok, R. G. Griffin, and S. Vega, *J. Chem. Phys.* **96**, 8624 (1992).
2. S. O. Smith, K. Aschheim, and M. Groesbeek, *Quart. Rev. Biophys.* **29**, 395 (1996).
3. M. Baldus, M. Tomaselli, B. H. Meier, and R. R. Ernst, *Chem. Phys. Lett.* **230**, 329 (1994).
4. M. Baldus and B. H. Meier, *J. Magn. Reson. A* **121**, 65 (1996).
5. G. J. Boender, J. Raap, S. Prytulla, H. Oschkinat, and H. J. M. de Groot, *Chem. Phys. Lett.* **237**, 502 (1995).

6. T. S. Balaban, G. J. Boender, A. R. Holzwarth, K. Schaffner, and H. J. M. de Groot, *Biochemistry* **34**, 15259 (1995).
7. R. R. Ernst, G. Bodenhausen, and A. Wokaun, "Principles of Nuclear Magnetic Resonance in One and Two Dimensions," Clarendon Press, Oxford (1987).
8. D. Marion and K. Wüthrich, *Biochem. Biophys. Res. Commun.* **113**, 967 (1983).
9. S. Vega, Dynamic magic angle spinning NMR spectroscopy, in "Nuclear Magnetic Resonance Probes of Molecular Dynamics" (R. Tycko, Ed.), p. 155, Kluwer, Dordrecht (1994).
10. Z. Luz, H. W. Spiess, and J. R. Titman, *Israel J. Chem.* **32**, 145 (1992).
11. A. F. de Jong, A. P. M. Kentgens, and W. S. Veeman, *Chem. Phys. Lett.* **109**, 337 (1984).
12. M. G. Munowitz and R. G. Griffin, *J. Chem. Phys.* **78**, 613 (1983).
13. A. Hagemeyer, K. Schmidt-Rohr, and H. W. Spiess, *Adv. Magn. Reson.* **13**, 85 (1989).
14. K. Schmidt-Rohr and H. W. Spiess, "Multidimensional Solid-State NMR and Polymers," Academic Press, New York, 1994.
15. G. Metz, X. Wu, and S. O. Smith, *J. Magn. Reson. A* **110**, 219 (1994).
16. A. E. Bennett, C. M. Rienstra, M. Auger, K. V. Laksmi, and R. R. Griffin, *J. Chem. Phys.* **103**, 1 (1995).
17. T. Gullion, D. B. Baker, and M. S. Conradi, *J. Magn. Reson.* **89**, 479 (1990).